

The velocity field of 2MRS, $K_s=11.75$ galaxies: constraints on β and bulk flow from the luminosity function

Enzo Branchini^{1,2,3}, Marc Davis⁴, Adi Nusser⁵

¹Dipartimento di Fisica “E. Amaldi”, Università degli Studi “Roma Tre”, via della Vasca Navale 84, 00146, Roma, Italy

²INFN Sezione di Roma Tre

³INAF, Osservatorio Astronomico di Brera, Milano, Italy

⁴Departments of Astronomy & Physics, University of California, Berkeley, CA. 94720

⁵Physics Department and the Asher Space Science Institute-Technion, Haifa 32000, Israel

23 October 2018

ABSTRACT

Using the nearly full sky $K_s = 11.75$ 2MASS Redshift Survey [2MRS] of $\sim 45,000$ galaxies we reconstruct the underlying peculiar velocity field and constrain the cosmological bulk flow within $\sim 100 \text{ h}^{-1}\text{Mpc}$. These results are obtained by maximizing the probability to estimate the absolute magnitude of a galaxy given its observed apparent magnitude and redshift. At a depth of $\approx 60 \text{ h}^{-1}\text{Mpc}$ we find a bulk flow $\mathbf{v}_B = (90 \pm 65, -230 \pm 65, 50 \pm 65) \text{ km s}^{-1}$ in agreement with the theoretical predictions of the Λ CDM model. The reconstructed peculiar velocity field \mathbf{v} that maximizes the likelihood is characterized by the parameter $\beta = 0.323 \pm 0.08$. Both results are in agreement with those obtained previously using the $\sim 23,000$ galaxies of the shallower $K_s = 11.25$ 2MRS survey.

In our analysis we find that the luminosity function of 2MRS galaxies is poorly fitted by the Schechter form and that luminosity evolves such that objects become fainter with increasing redshift according to $L(z) = L(z=0)(1+z)^{+2.7 \pm 0.15}$.

Key words: Cosmology: large-scale structure of the Universe, dark matter, cosmological parameters

1 INTRODUCTION

Peculiar velocities arising from the cosmological growth of density fluctuations affect the estimation of the distances and luminosities of extragalactic objects from their measured redshifts, a spurious effect commonly known as *redshift space distortions*. The effect is expected to be systematic because of the large scale coherence of the peculiar velocity field in the Λ CDM model. In this respect, redshift space distortions provide a unique tool to validate the Λ CDM and gravitational instability scenarios, to probe the underlying the velocity field and to estimate the growth rate of cosmological simulation $f(z) = \frac{d \ln D}{d \ln a}$, where z is the redshift, $a = (1+z)^{-1}$ is the expansion parameter and D is the linear growth factor. The growth rate f mainly depends on the mass density parameter Ω and the redshift (Peebles 1980). The exact dependence is determined by the underlying theory of gravity. Therefore the estimation of $f(z)$ constitutes a sensitive test to Einstein’s General Relativity.

The availability of large and relatively deep galaxy redshift surveys in recent years has triggered a strong interest on the apparent anisotropy in galaxy clustering induced by redshift distortions since they can be used to tighten constraints over different cosmological parameters (Amendola et al. 2005) and that to provide a unique way to discriminate between a dark energy scenario and a modified gravity theory (Guzzo et al. 2008; Zhang et al. 2008).

Redshift space distortions in the galaxy distribution at different epochs are now regarded as one of the most effective ways to attack the dark energy problem and constitutes one of the main scientific goals of generation redshift surveys like BigBoss (Schlegel et al. 2011) or Euclid (Laureijs et al. 2011).

Redshift distortions not only misplace galaxies. They also affect the estimate of the objects’ luminosities. And yet, little attention has been given to this second aspect of the same phenomenon. In fact, the idea of using systematic biases in the estimated galaxy luminosities to constrain peculiar motions is not new. It dates back to the work of Tammann et al. (1979) who correlated the magnitudes of nearby galaxies with their redshifts to constrain the velocity of the Virgo cluster relative to the Local Group. However, the method requires a large number of objects to be effective. For this reason several authors focused on average quantities rather than single objects. For example Baleisis et al. (1998); Blake & Wall (2002); Itoh et al. (2010) (and references therein) have exploited the Compton-Getting effect and searched for dipole variation in the surface number density of distant galaxies to estimate the bulk flow. Similarly, Abate & Feldman (2011) looked for a dipolar modulation in the variation of a suitably defined average apparent magnitude across the sky. Currently available all-sky redshift surveys, like 2MRS, allow an estimate of galaxy luminosities for a large num-

ber of galaxies. In this case, peculiar motions can be inferred from systematic variations in the estimated galaxy luminosities across the sky. Nusser et al. (2011) adopted this approach and showed that it can be used to estimate the bulk flow in the local universe. Nusser et al. (2012) took a step further and showed that the same idea could be used to constrain the growth rate of density fluctuations in the local universe, i.e. at $z \sim 0$.

In this paper we use the new redshift survey of nearly full-sky 2MASS Redshift Survey (2MRS) of ~ 45000 galaxies with $K_s \leq 11.75$ (Huchra et al. 2011) to supersede the work of Nusser et al. (2011) and Nusser et al. (2012) based on the previous release with a brighter apparent magnitude cut $K_s = 11.25$. The aim is twofold. First of all, there is a considerable interest in large-scale flows with some controversial claims of anomalous bulk flows on various scales that would exceed Λ CDM prediction (see e.g. Feldman et al. (2010); Kashlinsky et al. (2012) and reference therein), that were not confirmed by subsequent analyses (Nusser & Davis (2011); Bilicki et al. (2011); Nusser et al. (2011); Turnbull et al. (2012); Osborne et al. (2011); Mody & Hajian (2012)). It is an intriguing issue that certainly justifies a closer look. Our technique provides a fresh approach to this outstanding problem. Thanks to the improved dataset we should be able to detect significant departures from Λ CDM predictions within $100 \text{ h}^{-1}\text{Mpc}$. Second of all, our technique constrains the velocity field independently on distance indicators. As such, it is free of potential systematic errors arising from a miscalibration of the distance indicators. From the spatial distribution and estimated luminosities of 2MRS galaxies we are able to model the linear velocity field and determine its only free parameter, $\beta \equiv f(\Omega)/b$, where b is the linear bias parameter of the galaxy sample. Our aim is to improve the accuracy of the estimate obtained by Nusser et al. (2012) and constrain the fundamental quantity $f(\Omega)$ at $z \sim 0$.

Our method heavily relies on the estimation of the galaxy luminosity function [LF]. Therefore we take special care in detecting, evaluating and correcting for systematic biases related to the measurement of the LF. For this purpose we use a suite of different methods, some of which completely new, to estimate the LF and the selection functions of the sample. Since velocities are estimated at the redshifts of the objects, our results are probe to the so-called Kaiser rocket effect. Any method aimed at estimating the underlying mass density field from a spatial distribution of mass tracers in a redshift survey should take this correction into account. Therefore, we perform this correction and, in Appendix, we offer an analytic treatment of the effect.

The structure of the paper is as follows. In Section 2 we describe the theoretical tools used in this work: the maximum likelihood method and the different LF estimators used in the analyses. In Section 3 we describe the real and simulated datasets. In Section 4 we introduce, implement and apply a novel technique to estimate the selection function of the catalog directly from the observed redshift distribution of the galaxies. The results are compared with those obtained in Section 5 in which we first compute the LF and by integration, we obtain the selection function. In Sections 6 and 7 we apply our maximum likelihood method to estimate the bulk flow and the β parameter. Finally, in Section 8 we discuss and summarize our main results.

2 THEORETICAL TOOLS

The scope of this work is to use the 2MRS flux limited at $K_s = 11.75$ to estimate the cosmological bulk flow in the local uni-

verse and trace the underlying peculiar velocity field. Peculiar velocities contribute to the measured redshift of an object. If r is the proper distance of a galaxy, z its redshift and v is the line of sight component of its peculiar velocity, then $s \equiv cz = r + v$, where all quantities are expressed in km s^{-1} , including the speed of light c . The absolute magnitude is estimated from the apparent magnitude, m , through $M_0 = m - 15 - 5 \log cz$. The "observed" magnitude is different from the true one $M = m - 15 - 5 \log r_l = M_0 - 5 \log(1 - v/cz)$, where $r_l = r(1 + z)$ is the luminosity distance. The difference between M and M_0 can be used to infer the peculiar velocity of the object. This can be done by maximizing the probability $P(M_0|cz, \mathbf{v})$ of a galaxy having an observed magnitude M_0 given its redshift cz and peculiar velocity \mathbf{v} :

$$P(M_0|cz, \mathbf{v}) = \frac{\Phi(M)}{\int_{-\infty}^{M_l} \Phi(M) dM}, \quad (1)$$

where $\Phi(M)$ is the luminosity function, $M_l = m_l - 25 - 5 \log r_l$, the apparent magnitude limit of the catalog is $m_l = K_s = 11.75$ and the expression is valid as long as errors in the measured redshifts are small ($\sigma_{cz}/cz \ll 1$).

2.1 Bulk flow from magnitudes and redshifts

Nusser et al. (2011) presented a simple method to measure cosmological bulk flows by minimizing systematic variations in the galaxy magnitudes estimated from the observed redshifts.

The method can be illustrated by the following example. Let us assume that the peculiar velocity field is characterized by a bulk flow \mathbf{v}_B and galaxies have a Schechter LF (Schechter 1980):

$$\Phi(L) = 0.4 \ln(10) \Phi^* \left(\frac{L}{L_*} \right)^{1+\alpha} \exp\left(-\frac{L}{L_*}\right). \quad (2)$$

In the large distance and small redshift error approximation the probability in Eq. 1 is

$$P(L_0|cz; \mathbf{v}_B) = \frac{0.4 \ln(10) \left(\frac{\tilde{L}_0}{L_*} \right)^{1+\alpha} e^{-\tilde{L}_0/L_*}}{\Gamma(1+\alpha, \tilde{L}_l/L_*)}, \quad (3)$$

where $\tilde{L}_0 = (1 - 2\mathbf{v}_B/cz)L_0$ and $\tilde{L}_l = (1 - 2\mathbf{v}_B/cz)L_l$ and absolute magnitudes are related to luminosities through $M = -2.5 \log L + \text{const}$.

The presence of a bulk flow \mathbf{v}_B systematically increases or decreases the estimated luminosity of a galaxy L_0 . Therefore, an estimate of the bulk flow can be obtained by maximizing the probability $P(L_0|cz; \mathbf{v}_B)$ with respect to \mathbf{v}_B . It is trivial to generalize this approach to a generic form of the luminosity function.

This method can be seen as a generalization of the maximum likelihood approach proposed by Itoh et al. (2010). In that case the bulk flow was estimated from the apparent dipole anisotropy modulation in the surface number density of galaxies in the the SDSS-DR6 catalog, (Adelman-McCarthy et al. 2008). To estimate the bulk flow that method requires angular positions, apparent magnitudes and the photometric redshift of the galaxies. The method proposed here requires more information (spectroscopic redshifts) but allows an estimate of the bulk flow from a differential quantity, the LF, rather than an integral one (the number density of objects). As a result, this method is more sensitive to bulk flows than the one proposed by Itoh et al. (2010). A similar method that does not use spectroscopic redshifts but only apparent magnitudes has been recently proposed by Abate & Feldman (2011). In that case

the authors looked for systematic, dipole-like variations in the apparent magnitude of the LRGs in the SDSS survey (Eisenstein et al. 2001)).

2.2 β from magnitudes and redshifts

Nusser et al. (2012) have extended the maximum likelihood technique discussed above to constrain the full linear velocity field \mathbf{v} . The method requires redshifts, angular positions and apparent magnitudes of galaxies. Galaxy positions are given in redshift space and are used to compute the linear velocity field as a function of β . Details of the computation of the linear velocity field can be found in Nusser & Davis (1994). Predicted velocities are used to compute distances and estimate the true absolute magnitude of the objects. The best fit value of β is found by maximizing the probability $P(M_0|cz, \mathbf{v}(\beta))$ over all galaxies in the sample.

We stress that the linear velocity field is predicted from the galaxy distribution in redshift space. Such a procedure is prone to the so-called Kaiser rocket effect, a systematic error induced by estimating the selection function of galaxies using redshifts rather than distances. In this work we explicitly correct for this bias. A detailed treatment of the effect can be found in Appendix A.

2.3 Estimators of the galaxy luminosity function

The measurement of the LF represents a key step in the maximum likelihood methods outlined above. To guarantee an accurate measurement and to minimize possible systematic errors we have used different estimators for the luminosity function, $\Phi(M)$, that we briefly describe below.

- $1/V_{\text{Max}}$ estimator [Φ_V]. This simple non-parametric estimator originally proposed by Schmidt (1968) weights each object by the maximum observable comoving volume in which it can be detected. It is the only estimator among those we have considered that is sensitive to large scale inhomogeneities in the galaxy distribution.

- STY estimator [Φ_{Sch}]. This estimator has been originally proposed by Sandage et al. (1979). It assumes a Schechter form for $\Phi(M)$ (Schechter 1980) and computes the best fit parameters by maximizing the product of the probabilities for galaxies to have a magnitude M given the observed redshift z (Eq. 1):

$$P_s = \Pi_i P(M_i|z_i). \quad (4)$$

For a Schechter form

$$\begin{aligned} \Phi(M) &= 0.4 \ln(10) \Phi^* 10^{0.4(\alpha+1)(M_*-M)} \\ &\times \exp\left(-10^{0.4(M_*-M)}\right) \end{aligned} \quad (5)$$

The free parameters are M_* and α and the normalization Φ_* . The latter does not concern us here.

- Stepwise estimator [Φ_{Stpl}]. This method, originally proposed by Efstathiou et al. (1988), is non-parametric and has been derived from a maximum likelihood approach. The unknown luminosity function $\Phi(M)$ is discretized into $N_b - 1$ magnitude bins over the range $M_1 < M_2 \dots < M_{N_b}$ so that

$$\Phi(M) = \Phi_i \quad \text{for } M_{i+1} \geq M > M_i. \quad (6)$$

Given this stepwise form for $\Phi(M)$, the probability in Eq 1 becomes

$$P(M_i|z_i) = \frac{\Phi_i}{(M_l - M_j)\Phi_j + \Delta M \sum_{k < j} \Phi_k}. \quad (7)$$

where we take $M_{i+1} - M_i = \Delta M = \text{const}$ and assume that the actual and limit magnitudes, M and $M_l(z)$, fall into the bins i and j , respectively. The N_b free parameters Φ_i are estimated by maximizing the product of single galaxies' probabilities.

- Spline based estimator [Φ_{Spl}]. The maximum likelihood method used to constrain the velocity field \mathbf{v} requires a smooth LF in input. For this reason we introduce a new estimator in which the unknown LF is approximated by a smooth piecewise function

$$\Phi(M) = q_i(M) \quad \text{for } M_{i+1} \geq M > M_i, \quad (8)$$

where q_i is a third degree polynomial satisfying the boundary conditions $q_i(M_i) = \Phi_i$ and $q_i(M_{i+1}) = \Phi_{i+1}$ and defined such that its second derivative $d^2\Phi/dM^2$ is continuous over the magnitude range $M_1 - M_{N_b}$. The coefficients of the splines can be efficiently computed using the standard techniques described in Press et al. (1992). Splines can be integrated to estimate the denominator in Eq. 1 and the coefficients Φ_i are determined by maximizing the product of probabilities $P_s = \Pi_j P_j(M_j|z_j)$ extended to all galaxies in the sample. Splines obtained from this procedure may produce a noisy LF especially at the faint and bright end due to the limited number of objects. In order to suppress these spurious wiggles we maximize a function which is the sum of $\log[P_s]$ and a penalty function which acquires very large negative values when the third derivative of the splines is large. This procedure efficiently suppresses the wiggles and still yields a set of best fit coefficients Φ_i based on maximum likelihood considerations.

3 DATASETS

We use the recently compiled 2MRS catalog that contains all galaxies brighter than $K_s = 11.75$ with measured spectroscopic redshift selected from the 2MASS XSC catalog of nearly one million objects (Huchra et al. 2011). The catalog is 97.6 % complete and mostly unaffected by interstellar extinction and stellar confusion over the region $|b| > 5^\circ$ for $30^\circ \leq l \leq 330^\circ$ and $|b| \geq 8^\circ$ otherwise. The total sky coverage is over 91 %. The catalog contains about 43,000 galaxies and therefore represents a significant improvement over the $K_s \leq 11.25$ redshift catalog of 23,000 objects used in the Nusser et al. (2011) and Nusser et al. (2012) analyses.

Although the catalog extends out to $s \sim 30,000 \text{ km s}^{-1}$ we restrict our analysis to objects at smaller distances. To minimize incompleteness for nearby objects we consider a semi-volume limited sample that contains all galaxies with $s > s_{\text{cut}}$ and galaxies with $s \leq s_{\text{cut}}$ that, if placed at s_{cut} , would be brighter than the magnitude limit. We set $s_{\text{cut}} = 3,000 \text{ km s}^{-1}$. The semi volume limited catalog is therefore obtained by excluding all galaxies with $M > M_l(s_{\text{cut}}) = m - 5 \log r_l(s_{\text{cut}}) - 25$ and $s < s_{\text{cut}}$. In addition, throughout the paper we work with a version of the survey with collapsed fingers-of-god in the main nearby clusters and with the masked region near the galactic plane filled at a given redshift by folding the the positions of galaxies

In addition to the real catalog we will also consider a suite of mock 2MRS catalogs. They will be used to test the validity of our likelihood approach and assess its uncertainties. Indeed we have used two different sets of mock catalogs:

- Mock catalogs used to test the bulk flow accuracy [$\mathbf{v}_{\mathbf{B}}$ -Mocks]:

These mock catalogs are the same as Nusser et al. (2011). The set is composed by 200 semi-volume limited mock catalogs with $s_{\text{cut}} = 3,000 \text{ km s}^{-1}$ which contain the same number of objects as the real sample. Mock galaxies are randomly distributed within a

sphere of $200 \text{ h}^{-1} \text{ Mpc}$. Their absolute magnitudes are assigned according to the LF of 2MRS (early + late type) galaxies estimated by Westover (2007). Redshifts of the objects are the sum of the Hubble flow and peculiar velocities modeled as a random component sampled from a Gaussian distribution with zero mean and width of 300 km s^{-1} . This scatter accounts for the combined effect of small scale velocity dispersion and errors in the measured redshift. No underlying large scale bulk flow was assigned to the mock galaxies.

- Mock catalogs used to test the β accuracy [β -Mocks]:

These mocks are the same ones used in Nusser et al. (2012). They are a set of 135 2MRS mock catalogs extracted from the mock Two Micron All Sky Survey extracted from the Millennium simulation. Mock galaxies were obtained the semi analytic model of Springel et al. (2005); De Lucia & Blaizot (2007). In these mocks the central observer is not chosen at random. Instead, it is selected to match the density and the dynamical properties of our Local Group of galaxies. For our purposes the main relevant properties of the mock galaxies is their LF that is well approximated by a Schechter form. More details on the mock 2MRS galaxies can be found in Davis et al. (2011).

4 REDSHIFT DISTRIBUTION OF 2MRS GALAXIES AND THEIR EVOLUTION

The blue histogram in figure 1 shows the redshift distribution of objects in the semi-volume limited catalog of 2MRS galaxies, dN/ds . We use constant redshift bin of size $\Delta s = 150 \text{ km s}^{-1}$. Errorbars represent the Poisson scatter in each bin $\sigma_N = \sqrt{N} = \sqrt{dN/ds \times \Delta s}$. The black, continuous curve is a parametric fit to the distribution

$$\frac{dN}{ds} = AS(s)s^2, \quad (9)$$

where $S(s)$ is the galaxy selection function, i.e. the fraction of galaxies in the catalog at redshift s . The selection function can either be measured directly from the observed counts (Kirshner et al. 1979; Davis & Huchra 1982) or estimated from the LF. In this paper we adopt both approaches. In this section we use the first one and compare the result with the alternative approach in the next Section. For this purpose we present a novel method, the F/T estimator, in which the selection function is computed by integrating the following equation

$$\frac{d \ln S(s)}{ds} \Delta s = -\frac{F(s)}{T(s)}, \quad (10)$$

where $T(s)$ is the number of galaxies with redshift smaller than s that could also be detected at larger distances while $F(s)$ is the number of galaxies within s that can only be detected out to $s + \Delta s$. The normalization A is set by matching the total number of galaxies in the catalog within $s = 12,000 \text{ km s}^{-1}$. This estimator assumes that the galaxy luminosity and selection functions do not depend on the environment.

In Fig. 1 we compare the smooth redshift distribution of galaxies obtained from the selection function estimated with the F/T method (black continuous curve) is compared with the observed dN/ds (blue histogram). The curve fits the data well out to $s = 10,000 \text{ km s}^{-1}$. At higher redshifts the F/T method overestimates the observed number of galaxies. If real, this difference would indicate that we are located within an under-dense region extending out to $\sim 20,000 \text{ km s}^{-1}$. Alternatively, the mismatch can

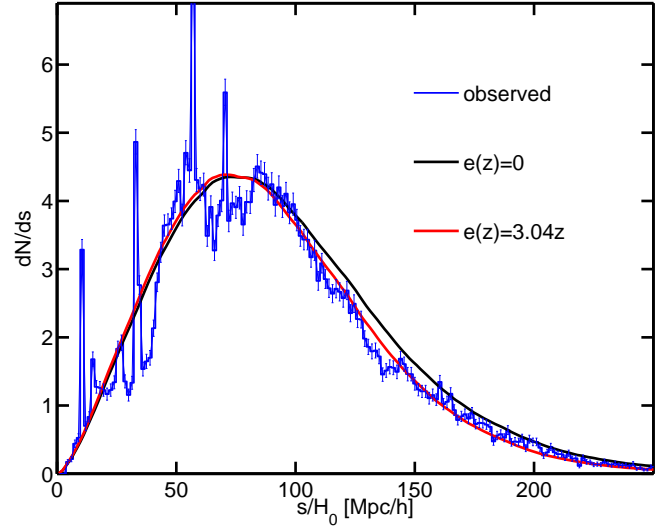


Figure 1. The blue histogram represents the observed redshift distribution of 2MRS galaxies computed in redshift bins $\Delta s = 150 \text{ km s}^{-1}$. Errorbars represent 1σ Poisson uncertainties. Continuous lines show the fits to the data obtained from the selection function computed using the F/T estimator. The black curve assumes Kochanek et al. (2001) k -correction but no luminosity evolution. The red curve shows the effect of k -correction a luminosity evolution $e(z) = 3.04z$.

hint some systematic errors is affecting the data. Before considering the first option, let us consider the possible sources of systematic uncertainties. To estimate the ratio $F(s)/T(s)$ in Eq. 10 one needs to compute the rest-frame absolute magnitude of galaxies, i.e. to apply the so-called k -correction, $k(z)$. In addition, the galaxy luminosity may evolve with time according to some law, $e(z)$. We correct for these systematic effects in our magnitude estimation as follows:

$$M = m - 25 - 5 \log r_l(z) - k(z) - e(z). \quad (11)$$

In the K_s band and at low redshift ($z < 0.25$) the k -correction is negative.¹ For 2MRS galaxies Kochanek et al. (2001), have found that $k(z) = -6 \log(1+z)$, a corrections that we adopted in this work. The evolution correction is more uncertain. It can be estimated by forcing a good match between the black curve and the histogram in Fig. 1. In practice we assume simple luminosity evolution model $L(z) = L(z=0)(1+z)^\epsilon$ and find ϵ by minimizing the χ^2 function

$$\chi^2 = \sum_{i=1}^{N_{bins}} \frac{1}{\sigma_{n,i}^2} \left[\frac{dN}{ds} - AS(s)s^2 \right]_i^2, \quad (12)$$

where the summation is over all redshift bins and σ_n is the Poisson noise in the galaxy counts. We obtain $L(z) = L(z=0)(1+z)^{+2.7 \pm 0.15}$. The result of this correction is represented by the solid, red line in Fig. 1, which indeed provides a good fit to observations.

5 THE LUMINOSITY FUNCTION OF 2MRS GALAXIES

In this section we use the different estimators described in Section 5 to compute the LF of the 2MRS galaxies and compare the

¹ Since the K_s band is on the Rayleigh Jeans part of the spectrum, and assuming the galaxy has little warm dust, $k(z)$ is negative, unlike the optical bands.

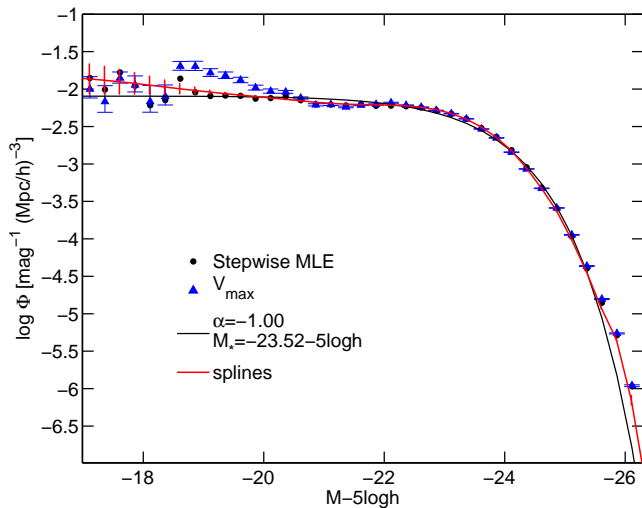


Figure 2. LFs of 2MRS galaxies obtained from the different estimators described in the text. Φ_V : blue triangles. Φ_{Sch} : Black, continuous curve. Φ_{Stp} : black dots. Φ_{Spl} : red, continuous line. Errorbars represent 1- σ bootstrap errors. Luminosity functions are computed in bins 0.25 mag. Symbols are plotted in every other bin for clarity.

results to assess their robustness. Absolute magnitudes were computed in redshift space using the $k(z)$ and $e(z)$ corrections described above. LFs are estimated in bins of 0.25 mag. The results are plotted in Fig. 2. All LFs are normalized to match the number of galaxies in the bin at $M = -23.37$ which is close to the value of $M_* = -25.52 - 5 \log h$ obtained from the Schechter fit.

In the plot the blue triangles represent the LF obtained using the $1/V_{MAX}$ method which is sensitive to large scale inhomogeneities. There is an excess of faint ($M_{K_s} > -20 + 5 \log h$) objects that we interpret as an overdensity in the number of galaxies in the nearby ($s < 2,200 \text{ km s}^{-1}$) volume of the universe. The black, thin curve shows the Schechter LF with best fit parameters ($\alpha = -1.0, M_* = -25.52 - 5 \log h$). At the bright end this fit deviates significantly from the others. This is not surprising and reflects that fact that we are forcing a Schechter fit to the LF of a composite sample of early and late type galaxies when we know that the two subsamples are well fitted by two different Schechter forms (Westover 2007) with M_* for early type objects 0.5 magnitude brighter than for the late-type objects (Nusser et al. 2011). The results of the Φ_{Stp} (black dots) and Φ_{Spl} (continuous, red curve) estimators are consistent with each other and with those of Φ_V for relatively bright objects $M_{K_s} - 5 \log h < -20$, i.e. in a volume large enough for fluctuations in the number density of galaxies to be negligible.

Errorbars in the plot are estimated from a bootstrap resampling analysis based on 20 random catalogs obtained from the original one by replacing each galaxy with n_r objects, where n_r is drawn from a Poisson distribution function with mean unity. All LF estimators have been applied to the 20 bootstrap catalogs. The error bars represent the *rms* scatter among the catalogs. Bootstrap uncertainties turned out to be very close to Poisson errors.

LFs are estimated in redshift space. We do not expect that they are different from those measured in real space, i.e. placing each object at their true distances. The reason is that correction for peculiar velocities are of the order of $\langle (v/cz)^2 \rangle$, where the average is taken over all directions in the surveyed area. Since we are dealing with an almost all-sky survey the effect is expected to be negli-

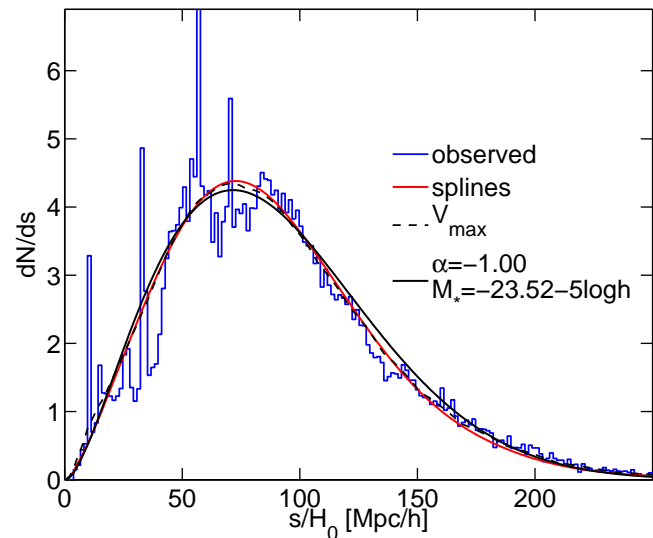


Figure 3. Redshift distribution of 2MRS galaxies. Blue histogram: same dN/ds as in Fig. 1. Curves: dN/ds predicted from different LF estimators. Black, continuous: Φ_{Sch} . Red, continuous: Φ_{Spl} . Black, dashed: Φ_V .

ble. To verify this hypothesis we have placed galaxies at their estimated true positions using the peculiar velocity model discussed in Section 7. We found no significant difference between the LFs estimated in real and redshift space.

From the estimated LF it is straightforward to compute the galaxy selection function:

$$S(s) = \frac{\int_{-\infty}^{M_I(s)} \Phi(M) dM}{\int_{-\infty}^{M_I(s_{cut})} \Phi(M) dM} \quad (13)$$

for $s > s_{cut}$. In Fig. 3, we show the dN/ds computed from the estimated selection function using Eq. 9. The different curves refer to different LF estimators. All of them are normalized to the observed galaxy counts (represented by the histogram) within $12,000 \text{ km s}^{-1}$.

The dN/ds curves obtained from Φ_{Sch} (black continuous), Φ_{Stp} (not plotted) and Φ_{Spl} (red continuous) are independent of the underlying inhomogeneities in the galaxy distribution unlike the one obtained from Φ_V (black, short-dashed) This difference is explains why the dN/ds obtained from the $1/V_{Max}$ estimator is different from the other curves both in the nearby region and in correspondence of the peaks of the distribution. The galaxy counts predicted from the Schechter LF are systematically larger above the observed one at $s > 10,000 \text{ km s}^{-1}$. This discrepancy reflects the fact that the Schechter fit underestimates the number of bright and faint objects alike (Fig. 2), resulting in an artificially small denominator in Eq. 13.

We notice the remarkable similarity between the dN/ds curves obtained from the spline and $1/V_{Max}$ estimators and the one obtained from the F/T method shown in figure 1. A result that further demonstrates the goodness of the new F/T estimator proposed in this paper.

From the estimated LFs it is straightforward to compute the mean galaxy overdensity within s :

$$1 + \langle \delta(< s) \rangle = \frac{\int_{-\infty}^{M_I(s)} \Phi(M) dM}{\int_{-\infty}^{M_I(s_{Norm})} \Phi(M) dM}. \quad (14)$$

The mean is set by the number density of galaxies within the red-

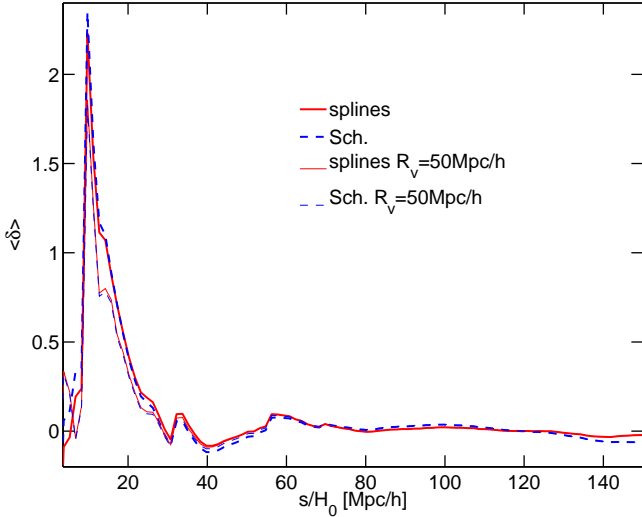


Figure 4. Mean galaxy overdensity (Y-axis) within the redshift s (X-axis) estimated from Φ_{Sch} (blue, dashed curves) and Φ_{Spl} (red, solid). Thick and thin curves indicate the two redshift cuts of 3,000 and 5,000 km s^{-1} applied to extract the semi-volume limited sample. All curves are normalized to $\langle \delta(s \leq 12,000 \text{ km s}^{-1}) \rangle = 0$.

shift $s_{Norm} = 12,000 \text{ km s}^{-1}$ chosen to normalize the selection function. The estimated cumulative overdensity obtained from the different LF estimators is plotted in figure 4. For the sake of clarity we only show the overdensity computed from the Schechter LF (thick, blue dashed line) and from the spline estimator (thin red) since the latter is very similar to those obtained from the $1/V_{Max}$ and the stepwise methods. The overdensity predicted by the two estimators are very similar within $s = 12,000 \text{ km s}^{-1}$. At larger distances, where the Schechter fit underestimates the number of expected counts, the corresponding overdensity is systematically smaller than obtained with the other estimators. These results depend on the choice of s_{cut} . Therefore we have repeated the analysis using a more aggressive cut $s_{cut} = 5,000 \text{ km s}^{-1}$. The results are shown by the thin curves in Fig. 4. Changing s_{cut} only affects the estimate of the overdensity in the inner region ($s < 3,000 \text{ km s}^{-1}$), as expected, but has no impact on the results obtained at larger radii.

6 MEASURING THE BULK FLOW FROM LF

We now apply the method described in Section 2.1 to the 2MRS $K_s < 1.75$ galaxy catalog to compute the bulk flow. Unlike Nusser et al. (2011) we do not break down the sample into early and late type objects since our best LF estimators Φ_{Spl} and Φ_{Ste} are designed to deal with a mixed population of objects. We take the LF estimated from Φ_{Spl} as the reference case and will test the sensitivity of the results to the choice of the estimator. We do not consider the Schechter LF since, as we have shown, it underestimates the abundance of bright galaxies.

We estimate the bulk flow in spherical shells of depth $\Delta s = 4,000 \text{ km s}^{-1}$ and out to $s = 10,000 \text{ km s}^{-1}$ by maximizing the probability function $P_s = \prod_i P_i(M_0|cz, \mathbf{v}_B)$, where the product is over all galaxies and P_i is the probability of the single object defined in Eq. ???. The binning in redshift and the volume sampled are the same as in Nusser et al. (2011) but the number of objects is twice as large. The results are displayed in Fig. ?. Points connected by lines represent the Cartesian components of the differ-

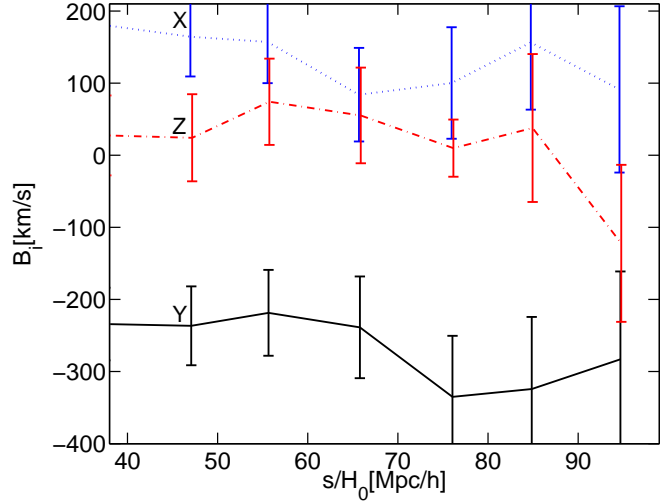


Figure 5. The bulk flow of 2MRS galaxies with $K_s < 12.75$ estimated from their luminosities in spherical shells 4,000 km s^{-1} -thick. The three Cartesian components are represented by a dotted (X), solid (Y) and dashed (Z) lines.

ential bulk flow estimated at the mean radius of each redshift shell. Different line styles are used for the different Cartesian components specified by labels. Errorbars show the rms scatter in the bulk flows estimated from the 200 \mathbf{v}_B -Mockes. These errors are contributed by shot noise, uncertainties in the observed magnitude and redshifts. They do not include cosmic variance. We find that the error budget is dominated by shot noise rather than redshift uncertainties. Errors in the measured magnitudes induce the same systematic errors in both the measured and the reference LFs and do not affect the bulk flow estimate. Not surprisingly, the results are remarkably robust to the method used to estimate the luminosity function: Φ_{Spl} and Φ_{Ste} and Φ_V . Finally, results are also robust to the k -correction and/or the evolution corrections adopted, as we have verified by switching off either corrections and yet obtaining very similar bulk flows.

Our results can be compared directly with those of (Nusser et al. 2011) and shown in Fig.1 of their paper. The two bulk flows are fully consistent with each other at all redshifts and for all Cartesian components. For example, at $R \approx 6,000 \text{ km s}^{-1}$ we find a bulk flow of $\mathbf{v}_B = (90 \pm 65, -230 \pm 65, 50 \pm 65) \text{ km s}^{-1}$, fully consistent with the one of (Nusser et al. 2011): $\mathbf{v}_B = (100 \pm 90, -240 \pm 90, 0 \pm 90) \text{ km s}^{-1}$. The fact that errors scale with the square root of the objects confirms that errors are dominated by Poisson noise.

7 MEASURING β FROM LF

In this section we apply the method described in Section 2.2 to model the linear velocity field traced by the 2MRS galaxies and to estimate the parameter β . The method uses the gravity field computed from the spatial distribution of the galaxies in the survey to minimize the scatter between the observed and the expected luminosity function. The result provides an estimate of β . The gravity field is computed from the spatial distribution of galaxies in redshift space using the linear method of Nusser & Davis (1994). As a reference luminosity function we use the one determined with the spline estimator assuming the luminosity evolution and k -correction discussed in Section 4. Since the velocity field is found by maximizing $P_s = \prod_j P_j(M_0|z, \mathbf{v}(\beta))$ with respect to β we need to produce a suite

of model velocity fields for different values of β . This is done by running the Nusser & Davis (1994) reconstruction procedure using different values of β in the range $[0.1, 1]$ in steps of 0.02.

The method is prone to several systematic errors:

- Since galaxy positions are given in redshift space, a direct estimate of the mass overdensity would systematically affect the predicted peculiar velocities. We correct for this so-called Kaiser rocket effect as described in Appendix A.
- To apply linear theory we need to filter out nonlinear contributions. For this purpose we first smooth the galaxy distribution with a Gaussian window of radius 400 km s^{-1} and then apply a second Gaussian filter of radius R_s to remove residual nonlinearities. We choose $R_s = 600 \text{ km s}^{-1}$ as a reference case and evaluate the robustness of the results to the choice of R_s .
- Linear theory recovers the flow pattern reasonably well up to $\delta \lesssim 1$, (Nusser et al. 1991; Branchini et al. 2002). For this reason Nusser et al. (2012) removed all galaxies in regions with overdensity above $\delta_{cut} = 1$ and verified that the results did not change significantly when a more conservative threshold $\delta_{cut} = 2$ was adopted. In our analysis we do not use any threshold and test the robustness of the results to overdensity cuts.

Given the model velocity field $\mathbf{v}(\beta)$ and the estimated galaxy luminosity function we apply the Nusser & Davis (1994) method to all galaxies within $10,000 \text{ km s}^{-1}$ and minimize $-\ln P_s = -\sum_i \ln P(M_{0i}|cz_i; \mathbf{v}(\beta))$ with respect to β . We do not consider objects beyond $10,000 \text{ km s}^{-1}$ due to the rapid decline in the observed number density of galaxies. In Fig. 6 we show the quantity $\Delta\chi^2 = -2\ln P_s(\beta) + 2\ln P_s(\beta_{min})$, where β_{min} is the best fit value of β found at the minimum of the curve. The width of the curve at $\Delta\chi^2 = 1$ provides an estimate of the 1- σ error. When all objects are considered (black, continuous curve) we find $\beta = 0.323 \pm 0.035$, to be compared with $\beta = 0.35 \pm 0.05$ found by Nusser et al. (2012). The errors quoted here are mainly contributed by shot noise, as confirmed by the scaling with the number of galaxies. However, other sources contribute to the error budget. We obtain more realistic errors by repeating the analysis on the 135 β -Mock catalogs. These errors include contributions from cosmic variance, nonlinear effects as well as shot noise. We find that cosmic variance and shot noise are similar in size and that the best fit estimate is $\beta = 0.323 \pm 0.083$.

To detect possible systematic errors and check the robustness of the results we have repeated the likelihood procedure changing the free parameters of the model.

- The method relies on the measurement of the galaxy LF. We have checked that the choice of the estimator has a negligible effect on the β value. This result is not surprising since, as shown explicitly in Nusser et al. (2012) the form of the luminosity function only affects the weighting given to galaxies in a certain luminosity range but has no impact on the value of the best fit β .
- The choice of galaxy evolution model adopted $e(z)$ might also affect the results. However, the effect is expected to be small since we only consider objects within $s = 10,000 \text{ km s}^{-1}$ where the effect of the evolution is small, as shown in Fig. 1. To verify this assumption we have repeated the analysis by switching off luminosity evolution, $e(z) = 0$. The results, shown by the red dotted curve in Fig. 6, confirm that the effect is negligible.
- To assess the impact of nonlinearities associated to the peaks of the density field we have repeated the analysis excluding all galaxies above $\delta_{cut} = 1$ and $\delta_{cut} = 2$, as in Nusser et al. (2012). We find no significant change in the best fit β value.

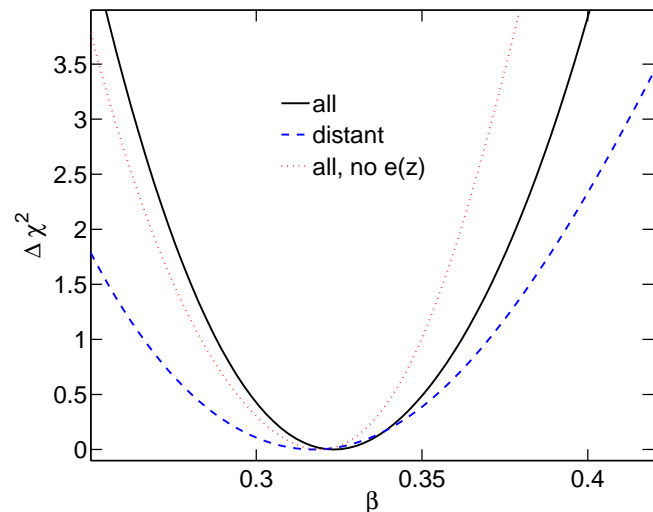


Figure 6. $\Delta\chi^2$ as a function of β . Solid line refers to all galaxies within $10,000 \text{ km s}^{-1}$ with magnitudes corrected for luminosity evolution. The best fit value is $\beta = 0.323 \pm 0.035$, where the quoted error is the width of the curve at $\Delta\chi^2 = 1$ and account for the finite number of galaxies. Red dashed curve: same galaxy sample but no correction for luminosity evolution. ($\beta = 0.319 \pm 0.033$). Blue dashed: subsample with galaxies at $s > 4,000 \text{ km s}^{-1}$. ($\beta = 0.317 \pm 0.05$).

- The smoothing radius R_s may also affect the estimate of β . Increasing the smoothing radius decreases the amplitude of the gravity field so that a larger value of β is required to fit the data. We have estimated the amplitude of the effect by increasing the Gaussian smoothing to $R_s = 1,000 \text{ km s}^{-1}$. The best fit value of β increases, as expected. However, the amplitude of this shift is ~ 3 times smaller than the random error.
- The catalog incompleteness for faint objects preferentially affects the innermost part of the sample. To minimize possible systematic errors we have repeated the analysis excluding all objects within $s = 4000 \text{ km s}^{-1}$. The result is illustrated by the blue, dashed curve in Fig. 6. The main effect is to increase shot-noise errors (by $\sim 40\%$) with a negligible shift in the best fit β .

8 DISCUSSION AND CONCLUSIONS

In this work we have used the new 2MRS galaxy catalog of galaxies brighter than $K_s = 11.75$ to estimate the peculiar velocity field and its bulk flow in the nearby ($s \leq 10,000 \text{ km s}^{-1}$) universe from the apparent brightening/dimming of galaxy luminosities. To do this we have used the same maximum likelihood techniques proposed by Nusser et al. (2011) and Nusser et al. (2012) and applied to the brighter 2MRS $K_s = 11.25$ sample, which contains about $\sim 50\%$ less objects. Since our technique heavily relies on the knowledge of the luminosity and selection functions of the galaxies, most of our efforts have been devoted in measuring accurately these quantities to keep possible systematic errors under control.

The main results of our analysis can be summarized as follows:

- We have computed the LF of 2MRS galaxies down to $M_{K_s} - 5\log h = -17$ using four different estimators to search for possible biases in the measured LF (see e.g. Ilbert et al. (2004)) and derived quantities. The LF obtained from the $1/V_{Max}$ estimator shows an excess of objects fainter than $M_{K_s} - 5\log h = -20$ not seen with

other estimators. We interpret this feature as large scale overdensity in the distribution of nearby ($cz < 2,200 \text{ km s}^{-1}$) galaxies since the $1/V_{Max}$ method is sensitive to large scale inhomogeneities.

Parametric estimators in which the LF is modeled with a Schechter form may induce systematic errors. More specifically, we find that the best fit Schechter form to the observed LF systematically underestimates the number density of bright ($M_{K_s} - 5 \log h < 25.5$) objects. This bias arises from fitting a single Schechter luminosity function to a composite sample of early and late type objects (Nusser et al. 2011). We have introduced a novel, non-parametric estimator for the LF similar to the stepwise method of Efstathiou et al. (1988) with the advantage of producing a smooth LF to be fed into the maximum likelihood method used in this work. Both the new estimator and the stepwise method hint at an excess of faint objects, quantified by a steepening of the LF in excess of the typical power-law slope $\alpha = -1.0$. The significance of this faint end excess, however, is barely above 1σ .

It turns out that the differences among the LFs estimated with various method are rather small and have no practical impact for our goals. That is to say that the bulk flow and the β values obtained from the maximum likelihood procedure do not significantly depend on LF estimator adopted.

- From the LFs we estimate the selection function of the catalog and the redshift distribution of the 2MRS galaxies. The results are compared with the observed dN/ds and with the redshift distribution obtained from a novel F/T estimator. This new statistical tools allows one to measure the selection function of the catalog from the observed redshift distribution of the galaxies, rather than from the LF. The F/T estimator systematically over predicts the number of objects in the outer part of the survey that we interpret as an evolution in the galaxy luminosity. According to this interpretation the galaxy luminosity evolves so that objects would grow fainter with the redshift. A simple luminosity evolution model $L(z) = L(z=0)(1+z)^{+2.7 \pm 0.15}$ is sufficient to fit to the observed dN/ds .

This result is not surprising since galaxy evolution in the infrared band can be significant even in the local patch of the universe. In the far infra red, evidence for an evolution in the number density of IRAS galaxies has been reported by a number of authors, although there is some controversy on the magnitude of the effect (see e.g. Oliver et al. (1992); Fisher et al. (1995); Springel & White (1998); Takeuchi et al. (2003) and reference therein). However, all these works find that the galaxy number density increase with redshift whereas in our case the positive evolution in luminosity would decrease the number density of objects selected above a given flux. This puzzling result, however, does not affect the outcome of our maximum likelihood methods since in our analysis we consider galaxies with $s < 10,000 \text{ km s}^{-1}$, where the evolution is found to be negligible.

- Our estimation of the bulk flow in the local ($s < 10,000 \text{ km s}^{-1}$) universe is fully consistent with that of Nusser et al. (2011). For example, at $R \approx 6,000 \text{ km s}^{-1}$ we find $\mathbf{v}_B = (90 \pm 65, -230 \pm 65, 50 \pm 65) \text{ km s}^{-1}$ to be compared with $\mathbf{v}_B = (100 \pm 90, -240 \pm 90, 0 \pm 90) \text{ km s}^{-1}$. In both cases errors are dominated by shot noise and which explains the $\sim 40\%$ improvement in the accuracy of the estimate. Cosmic variance is not included. This the most precise estimate of the bulk flow in the local universe obtained without using distant indicators. Among alternative bulk flow estimators, the one used here is arguably more precise than those proposed by Itoh et al. (2010) and Abate & Feldman (2011) since, in our case, we look for systematic variations in a differential quantity, the LF, rather than using

integral quantities. Our method is also superior to the one proposed by Haehnelt & Tegmark (1996) that exploits the kinetic Sunyaev-Zel'dovich CMB distortions along the line-of-sight to galaxy clusters (Sunyaev & Zeldovich 1980), due to the limited number of available galaxy clusters within $10,000 \text{ km s}^{-1}$. Indeed, the likelihood method proposed here is the idea tool to probe bulk flows at different locations in the universe from luminosity variations measured in deep and wide next generations redshift surveys (for a quantitative assessment see Nusser et al. (2011)).

Our estimate of the bulk flow agrees well with the recent estimates of the bulk flow of Nusser & Davis (2011) $\mathbf{v}_B(R \approx 6,000 \text{ km s}^{-1}) = (120 \pm 40, -250 \pm 40, 40 \pm 60) \text{ km s}^{-1}$, based on the SFI++ Tully-Fisher catalog of distance indicators (Masters et al. 2006; Springob et al. 2007; Davis et al. 2011). We also agree with the bulk flow obtained from SNe Ia data (Colin et al. 2011; Dai et al. 2011) and most notably with Turnbull et al. (2012) who used the high quality 'First amendment' dataset. Finally, our result also agrees with the recent analysis of the 2MASS galaxy dipole Bilicki et al. (2011). It is quite remarkable that consistent bulk flows have been obtained from different datasets and using different methods affected by different systematics and that all of them are in agreement with Λ CDM expectations.

- Using the gravity field computed from the spatial distribution of 2MRS galaxies we were able to obtain a linear model for the velocity field in the local universe by minimizing the scatter in the LF. From this procedure we obtain $\beta = 0.323 \pm 0.083$, in agreement with the results of Nusser et al. (2012) ($\beta = 0.323 \pm 0.1$). The increase in the accuracy is more modest than for the bulk flow since in this case the error budget is almost equally contributed by shot noise and cosmic variance, which is now accounted for. We did check that this result is robust to luminosity evolution, to the choice of the LF estimator, to catalog incompleteness for faint objects and to the smoothing scale used to remove nonlinearities. Our estimation of β is also in good agreement with that of Davis et al. (2011) obtained by comparing the gravity field of 2MRS $K_s < 11.25$ galaxies with the peculiar velocities in the SFI++ galaxy catalog ($\beta = 0.325 \pm 0.045$) and also with that of Bilicki et al. (2011) ($\beta = 0.38 \pm 0.04$) obtained from the 2MASS galaxy dipole.

From β it is possible to constrain the growth rate of density fluctuations $f(\Omega) = \beta/b$ if b can be determined independently. However measuring the galaxy bias from existing datasets is difficult and no theory of galaxy evolution is currently able to precisely constrain its value. Alternatively, one could estimate some parameter combination that does not depend on bias and yet provides the possibility of efficiently discriminating among different cosmological scenarios. The combinations $f(\Omega)\sigma_8 = \beta\sigma_{8,gal}$ provides such possibility since both β and $\sigma_{8,gal}$, the *rms* density contrast in galaxy number, can be measured from redshift surveys and $f(\Omega)\sigma_8$ is as good as $f(\Omega)$ to test alternative cosmological scenarios (White et al. 2009; Percival & White 2009; Song & Percival 2009). The validity of this probe relies on the hypothesis that at $8 \text{ h}^{-1} \text{ Mpc}$, the scale at which one measures $\sigma_{8,gal}$, galaxy bias has the same value as at the much larger scales in which one measures β . Estimates of $f(\Omega)\sigma_8$ from the apparent anisotropy in galaxy clustering have been obtained in the redshift range $z \approx [0.2, 0.8]$ (Percival et al. 2004; Samushia et al. 2012; Blake et al. 2011; Guzzo et al. 2008). Several authors have pointed out that an accurate estimate of the growth rate at $z \approx 0$, which can only be obtained from the peculiar velocity field in the local universe, would significantly increase the discriminatory power of this cosmological probe. The most recent estimates have been obtained

by Davis et al. (2011) ($f(\Omega)\sigma_8 = 0.31 \pm 0.06$ at $z < 0.033$) and Turnbull et al. (2012) ($f(\Omega)\sigma_8 = 0.4 \pm 0.04$ at $z \approx 0.02$). In our case, taking $\sigma_{8,gal} = 0.97 \pm 0.05$ from Westover (2007); Reid et al. (2010), we find $f(\Omega)\sigma_8 = 0.31 \pm 0.09$ for $z < 0.033$, in good agreement with the other results.

Since in many models of modified gravity the growth rate can be parametrized as $f(\Omega) = \Omega^\gamma$ (Linder 2005) many recent works have focused on comparing the estimated growth index γ with the canonical value $6/11$ of a Λ CDM universe. The value of γ from our estimate of $f(\Omega)\sigma_8$ must be consistent with those obtained from the estimates of Davis et al. (2011) Turnbull et al. (2012). The value obtained combining the two estimates ($\gamma = 0.616 \pm 0.052$ Hudson and Turnbull 2012, *ApJ submitted*) is consistent with the one obtained by Nusser & Davis (2011) from the bulk flow of SFI++ galaxies ($\gamma = 0.495 \pm 0.096$) and with those obtained from galaxy clustering on larger scales. All of them agree with a Λ CDM standard gravity model.

9 ACKNOWLEDGMENTS

This work was supported by THE ISRAEL SCIENCE FOUNDATION (grant No.203/09), the German-Israeli Foundation for Research and Development, the Asher Space Research Institute and by the WINNIPEG RESEARCH FUND. MD acknowledges the support provided by the NSF grant AST-0807630. EB acknowledges the support provided by MIUR PRIN 2008 'Dark energy and cosmology with large galaxy surveys' and by Agenzia Spaziale Italiana (ASI-Uni Bologna-Astronomy Dept. 'Euclid-NIS' I/039/10/0) AN thanks the Physics Department of the Roma Tre University for the kind hospitality.

APPENDIX A: THE KAISER ROCKET EFFECT

In this appendix we work out the expression for the so-called Kaiser rocket effect for two different types of catalogs: a flux limited and a volume limited redshift survey.

A1 Kaiser effect for a flux limited survey

Assume we have a flux limited redshift survey of galaxies with apparent magnitudes $< m_l$. The selection function $S(r)$ is proportional to the average density and, apart from a normalization factor, is defined as

$$S(r) \propto \int_{-\infty}^{M_l(r)} \Phi(M) dM \quad (\text{A1})$$

where $M_l = m_l - 15 \log(r_l) - 15$, r_l is the luminosity distance in km s^{-1} and $\Phi(M)$ is the galaxy luminosity function. Here, for convenience, we drop the subscript l from the luminosity distance. The mean number density of galaxies within r_n is defined as

$$\bar{n} = \frac{3}{4\pi r_n^3} \sum_{r_i < r_n} \frac{1}{S(r_i)}. \quad (\text{A2})$$

I assume that $S(r_n)$ is sufficiently large to avoid using the other estimator which has J_3 in it (that estimator minimizes the variance at the expense of biasing \bar{n}). The true density contrast in a cell of size ΔV at r is then

$$1 + \delta_t = \frac{1}{\bar{n}} \sum_{i \in \Delta V} \frac{1}{S(r_i)} = \frac{n_o}{\bar{n}} \frac{1}{S(r)}. \quad (\text{A3})$$

where $n_o \Delta V$ is the actual number of observed galaxies within ΔV and we have assumed that ΔV is so small that $r_i = r$.

Since we are given the redshift $s = r + u$ rather than distances, we can only compute S at the redshift position s_i of a galaxy. This will introduce a bias known as Kaiser rocket effect since it would induce a spurious component in the gravitational attraction estimated in redshift space. Note also that ΔV will change by the transformation to redshift space, which will amount to the usual redshift distortions. As a result, the estimated density contrast in redshift space is in A3,

$$1 + \delta = \frac{n_o}{\bar{n}} \frac{1}{S(r)} = \frac{n_o}{\bar{n}} \frac{1}{S(s)} \left(1 + \frac{1}{s} \frac{d \ln S}{d \ln s} u \right) = 1 + \delta_t \left(1 + \frac{1}{s} \frac{d \ln S}{d \ln s} u \right). \quad (\text{A4})$$

where $\frac{n_o}{\bar{n}} \frac{1}{S(s)}$ are directly determined from the data. The extra term involving the logarithmic derivative of S is the Kaiser term and can be evaluated at s instead of r when one assumes linear theory. Any method aimed at estimating the underlying mass density field from a spatial distribution of mass tracers in a redshift survey should take this correction into account.

A2 Kaiser effect for a volume limited survey

It is often assumed that Kaiser correction is negligible in a volume limited survey. We show here that this is not quite the case. Let us consider a volume limited survey of all galaxies that are bright enough to be seen out to a distance r_{max} , i.e. all these galaxies have $M < M_{l,v} = m_l - 5 \log(r_{max}) - 15$. The true density contrast at $r < r_{max}$ is

$$1 + \delta_t = \frac{n_o(r)}{\bar{n}}, \quad (\text{A5})$$

where \bar{n} is defined as $3N/(4\pi r_{max}^3)$ where N is the total number of galaxies in the volume limited survey. However, since we observe redshifts and not distances $r = s - u$, objects are selected according to their absolute magnitude estimated in redshift space $M_0 = m - 5 \log(s) - 15 \approx -5 \log(r) - 2.17(u/s) - 15$ and $M = m - 15 \log(r) - 15 \approx M_0 + 2.17(u/s)$. Thus, for example, in a volume element ΔV where u is positive, the physical limit $M_{l,v}$ is larger than its redshift-space estimate $M_{0,l,v}$. Therefore, for redshift space data, the mean number density within s is

$$n_o = \int_{-\infty}^{M_{l,v} + 2.17u/s} \Phi(M) dM. \quad (\text{A6})$$

where the integration extends out to $M_{l,v} + 2.17(u/s)$ instead of $M_{l,v}$. To correct for this effect the density contrast should be defined as

$$1 + \delta = \frac{n_o}{\bar{n}} \frac{\int_{-\infty}^{M_{l,v}} \Phi(M) dM}{\int_{-\infty}^{M_{l,v} + 2.17u/s} \Phi(M) dM} \quad (\text{A7})$$

$$= \frac{n_o}{\bar{n}} \frac{S(r_{max})}{S(r_{max} - u)} \quad (\text{A8})$$

$$\approx \frac{n_o}{\bar{n}} \left[1 + \left(\frac{1}{s} \frac{d \ln S}{d \ln r} \right)_{r_{max}} \frac{u}{r_{max}} \right] \quad (\text{A9})$$

where we have used the definition of S in Eq. A1. This is the analogous of the Kaiser correction for a flux limited survey except that u is multiplied by a quantity that is defined at r_{max} rather than at r . For the 2MRS $K_s < 11.75$ catalog, $d \ln S / d \ln r$ grows from 0.92 at $s = 3,000 \text{ km s}^{-1}$ to 1.42 at $5,000 \text{ km s}^{-1}$ and the corresponding Kaiser term in a sub-volume limited catalog cannot be neglected.

REFERENCES

- Abate A., Feldman H. A., 2011, ArXiv e-prints
- Adelman-McCarthy J. K., Agüeros M. A., Allam S. S., Allende Prieto C., Anderson K. S. J., Anderson S. F. e. a., 2008, *ApJS*, 175, 297
- Amendola L., Quercellini C., Giallongo E., 2005, *MNRAS*, 357, 429
- Baleisis A., Lahav O., Loan A. J., Wall J. V., 1998, *MNRAS*, 297, 545
- Bilicki M., Chodorowski M., Jarrett T., Mamon G. A., 2011, *ApJ*, 741, 31
- Blake C., Brough S., Colless M., Contreras C., Couch W., Croom S., Davis T., Drinkwater M. J., 2011, *MNRAS*, 415, 2876
- Blake C., Wall J., 2002, *Nat*, 416, 150
- Branchini E., Eldar A., Nusser A., 2002, *MNRAS*, 335, 53
- Colin J., Mohayaee R., Sarkar S., Shafieloo A., 2011, *MNRAS*, 414, 264
- Dai D.-C., Kinney W. H., Stojkovic D., 2011, *JCAP*, 4, 15
- Davis M., Huchra J., 1982, *ApJ*, 254, 437
- Davis M., Nusser A., Masters K. L., Springob C., Huchra J. P., Lemson G., 2011, *MNRAS*, 413, 2906
- De Lucia G., Blaizot J., 2007, *MNRAS*, 375, 2
- Efstathiou G., Ellis R. S., Peterson B. A., 1988, *MNRAS*, 232, 431
- Eisenstein D. J., Annis J., Gunn J. E., Szalay A. S., Connolly A. J., Nichol R. C., Bahcall e. a., 2001, *AJ*, 122, 2267
- Feldman H. A., Watkins R., Hudson M. J., 2010, *MNRAS*, 407, 2328
- Fisher K. B., Huchra J. P., Strauss M. A., Davis M., Yahil A., Schlegel D., 1995, *ApJS*, 100, 69
- Guzzo L., et al., 2008, *Nat*, 451, 541
- Haehnelt M. G., Tegmark M., 1996, *MNRAS*, 279, 545
- Huchra J. P., Macri L. M., Masters K. L., Jarrett T. H., Berlind P., Calkins M., Crook A. C. e. a., 2011, ArXiv e-prints
- Ilbert O., Tresse L., Arnouts S., Zucca E., Bardelli S., Zamorani G., Adami C., Cappi A., Garilli B., Le Fèvre O., Maccagni D., Meneux B., Scaramella R., Scodeggio M., Vettolani G., Zanichelli A., 2004, *MNRAS*, 351, 541
- Itoh Y., Yahata K., Takada M., 2010, *PhRvD*, 82, 043530
- Kashlinsky A., Atrio-Barandela F., Ebeling H., 2012, ArXiv e-prints
- Kirshner R. P., Oemler Jr. A., Schechter P. L., 1979, *AJ*, 84, 951
- Kochanek C. S., Pahre M. A., Falco E. E., Huchra J. P., Mader J., Jarrett T. H., Chester T., Cutri R., Schneider S. E., 2001, *ApJ*, 560, 566
- Laureijs R., Amiaux J., Arduini S., Auguères J., Brinchmann J., Cole R., Cropper M., Dabin C., Duvet L., Ealet A. e. a., 2011, ArXiv e-prints
- Linder E. V., 2005, *PhRvD*, 72, 043529
- Masters K. L., Springob C. M., Haynes M. P., Giovanelli R., 2006, *ApJ*, 653, 861
- Mody K., Hajian A., 2012, ArXiv e-prints
- Nusser A., Branchini E., Davis M., 2011, *ApJ*, 735, 77
- Nusser A., Branchini E., Davis M., 2012, *ApJ*, 744, 193
- Nusser A., Davis M., 1994, *ApJL*, 421, L1
- Nusser A., Davis M., 2011, *ApJ*, 736, 93
- Nusser A., Dekel A., Bertschinger E., Blumenthal G. R., 1991, *ApJ*, 379, 6
- Oliver S. J., Rowan-Robinson M., Saunders W., 1992, *MNRAS*, 256, 15P
- Osborne S. J., Mak D. S. Y., Church S. E., Pierpaoli E., 2011, *ApJ*, 737, 98
- Peebles P. J. E., 1980, The large-scale structure of the universe
- Percival W. J., Burkey D., Heavens A., Taylor A., Cole S., Peacock J. A., Baugh C. M., Bland-Hawthorn J., 2004, *MNRAS*, 353, 1201
- Percival W. J., White M., 2009, *MNRAS*, 393, 297
- Press W. H., Teukolsky S. A., Vetterling W. T., Flannery B. P., 1992, Numerical recipes in FORTRAN. The art of scientific computing
- Reid B. A., Percival W. J., Eisenstein D. J., Verde L., Spergel D. N., Skibba R. A., Bahcall N. A., Budavari T., Frieman J. A., Fukugita M., Gott J. R., 2010, *MNRAS*, 404, 60
- Samushia L., Percival W. J., Raccanelli A., 2012, *MNRAS*, 420, 2102
- Sandage A., Tammann G. A., Yahil A., 1979, *ApJ*, 232, 352
- Schechter P. L., 1980, *AJ*, 85, 801
- Schlegel D., Abdalla F., Abraham T., Ahn C. e. a., 2011, ArXiv e-prints
- Schmidt M., 1968, *ApJ*, 151, 393
- Song Y., Percival W. J., 2009, *JCAP*, 10, 4
- Springel V., White S. D. M., 1998, *MNRAS*, 298, 143
- Springel V., White S. D. M., Jenkins A., Frenk C. S., Yoshida N., Gao L., Navarro J., Thacker R., Croton D., Helly J., Peacock J. A., Cole S., Thomas P., Couchman H., Evrard A., Colberg J., Pearce F., 2005, *Nat*, 435, 629
- Springob C. M., Masters K. L., Haynes M. P., Giovanelli R., Marinoni C., 2007, *ApJS*, 172, 599
- Sunyaev R. A., Zeldovich I. B., 1980, *MNRAS*, 190, 413
- Takeuchi T. T., Yoshikawa K., Ishii T. T., 2003, *ApJL*, 587, L89
- Tammann G. A., Yahil A., Sandage A., 1979, *ApJ*, 234, 775
- Turnbull S. J., Hudson M. J., Feldman H. A., Hicken M., Kirshner R. P., Watkins R., 2012, *MNRAS*, 420, 447
- Westover M., 2007, PhD thesis, Harvard University
- White M., Song Y.-S., Percival W. J., 2009, *Mon. Not. Roy. Astron. Soc.*, 397, 1348
- Zhang H., Yu H., Noh H., Zhu Z.-H., 2008, *Physics Letters B*, 665, 319